ELSEVIER

Journal of Nuclear Materials 247 (1997) 215–221

journal of nuclear materials

Thermochemical modeling of actinide alloys related to advanced fuel cycles

T. Ogawa [a,*], M. Akabori [a], F. Kobayashi [a], R.G. Haire [b]

[a] *Japan Atomic Energy Research Institute, Tokai-mura, Naka-gun, Ibaraki-ken 319-11, Japan*
[b] *Oak Ridge National Laboratory, Oak Ridge, TN 37831-6375, USA*

Abstract

Innovative approaches for improved management of transuranium elements are being sought. The use of either metallic or nitride fuels, coupled with pyrochemical reprocessing techniques, are being studied. As our experience with these advanced fuels is limited, their development will be promoted by thermochemical analysis. This paper reviews our thermochemical modeling of technical problems related to advanced fuel cycles and presents models of the actinide alloys and nitrides together with experimental verification of these thermochemical predictions. © 1997 Elsevier Science B.V.

1. Introduction

With the amount of transuranium elements (TRU) being accumulated each year, innovative approaches for improved management of TRU are being sought. The use of either metallic or nitride fuels, coupled with pyrochemical reprocessing techniques, may provide safer fast reactors for actinide burning, more economical fuel cycles as well as the improved containment of hazardous and politically sensitive materials. As our experience with such advanced fuels is limited, their development will be promoted by acquiring knowledge and understanding of irradiation behaviors, fabrication methods and reprocessing techniques. Thermochemical analysis has become an important element in the development of advanced fuels and processes, particularly those involving the actinides.

2. Dense fuel cycle concepts and processes

A double-strata fuel cycle concept has been proposed for burning minor actinides (MA: Np, Am and Cm) separated from high-level waste (HLW) [1,2]. The MA coming from the commercial fuel cycle is confined in the second stratum, the actinide burner cycle and exit there only as fission products. Ideally MA from ten 3000 MW (~ 1000 MWe) LWR can fuel a 1000 MW reactor each year. With some modification, the concept may also be applied to plutonium burning or utilization depending on the energy strategy [3].

Actinides will be separated from HLW as nitrates. The nitrates are converted to solid oxides by a sol–gel technique. By adding carbon powder to the nitrate solutions, the mixture of carbon and metal oxides can be obtained. The latter mixture can be converted to mononitride fuels by a carbothermic synthesis in a nitrogen atmosphere. The nitride fuels would then be fed into a reactor dedicated for actinide burning, 'ABR: actinide burner reactor'. The irradiated fuels are pyrochemically reprocessed by molten-salt electrorefining.

An electrorefining process of the nitrides is being studied, where the nitrides are anodically dissolved and the actinide metals recovered on the cathode [4,5]. The metals are then converted to nitrides in a liquid cadmium bath. The nitridation in liquid cadmium has an attractive aspect: Further removal of lanthanides from actinides may be achieved if necessary (Fig. 1). Experiments examining the reaction of nitrogen with Cd–U–Ce–Gd liquid alloys [6] have shown that uranium is preferentially nitrided, followed by gadolinium, which, among the lanthanide fission

---

[*] Corresponding author. Tel.: +81-29 282 5430; fax: +81-29 282 6097; e-mail: ogawa@sun2sarl.tokai.jaeri.go.jp.

0022-3115/97/$17.00 © 1997 Elsevier Science B.V. All rights reserved.
PII S0022-3115(97)00047-0

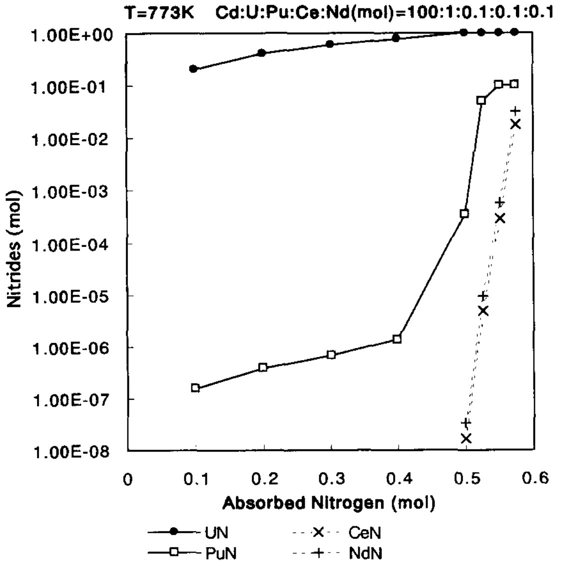

Fig. 1. Prediction on nitridation of actinides and lanthanides in liquid cadmium.

products, is less stable in liquid cadmium. Cerium was the last to react with nitrogen.

An alternative approach being studied is the direct nitridation of the actinides in a moltensalt bath, 'LINEX', instead of electrorefining (Figs. 2 and 3) [7]. The nitrides are anodically dissolved in a LiCl–KCl–$CdCl_2$ melt. The nitrogen evolved during dissolution is trapped by lithium to form Li_3N, which is then returned to the molten salts. Actinides preferentially segregate in the melt as nitrides by the methathetical reaction with Li_3N. The alkali and the alkaline earth metals and the most of the rare earth fission products would remain in the salt phase. Further addition of Li_3N would remove the rare earths from the salt phase to prevent excessive accumulation of them. (Li_3N may be also used as a nitriding agent in the liquid Cd process mentioned above, since cadmium decomposes Li_3N. The use of Li_3N may give an improved mass balance in the process rather than passing nitrogen gas in liquid Cd.)

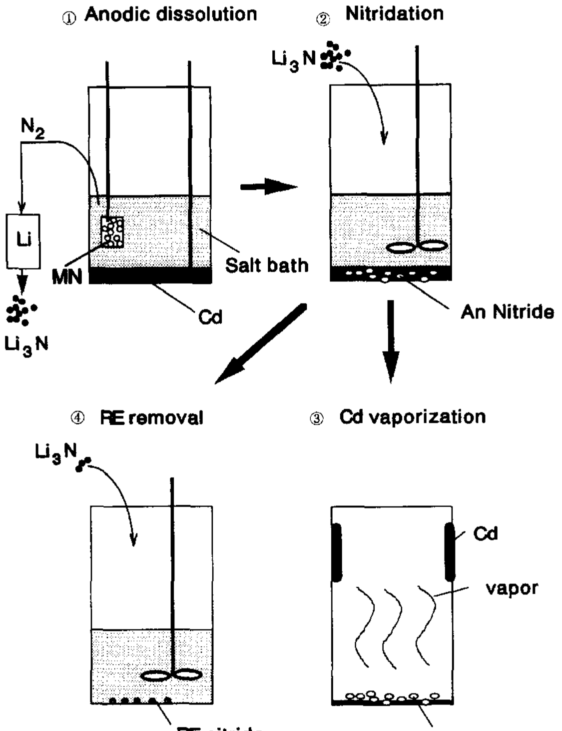

Fig. 2. Outline of LINEX process: Li_3N extraction of actinides in molten salts. (An: actinides. RE: rare earths.)

Thermochemical predictions have been made basis for the development of the above processes. A generic thermochemical datafile, An–Ln–Cd–Li–K–Cl–N, is being prepared for this purpose. The file takes into account molten chlorides, nitrides, actinide alloys, liquid cadmium alloys as well as intermetallics between cadmium and lanthanides/actinides. The electrorefining process, for in-

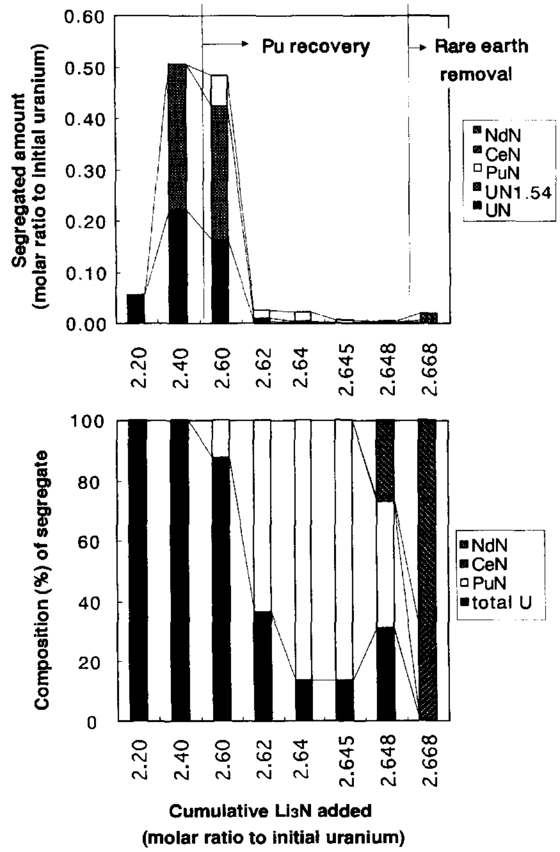

Fig. 3. Prediction on LINEX process on a LiCl–KCl molten salt containing U:Pu:Ce:Nd = 1:0.1:0.006:0.014. Extra Li_3N is expended for the reaction with cadmium metal in the system, but the liberated N_2 can be recovered.

stance, can be solved in the same theoretical framework where the problem of component redistribution in the irradiated fuel is treated: thermochemistry determines the local equilibrium at the interface of the different phases and the rest of the problem is dealt by the numerical calculation of the diffusion processes.

It is not possible to state with confidence, that fabrication and reprocessing of MA-containing fuels are technically feasible, as several potential problems remain. One must be concerned with the product yields at every stage of the fuel cycle. If extremely high yields cannot be achieved, it would not make sense to recycle MA or even plutonium to reduce environmental impact. At the same time, the material balances have to be closely traced and controlled. The present status of our efforts in the thermochemical modeling and related experimental studies is discussed in this paper.

3. Modeling of actinide solution phases

Thermochemical problems can be reduced to the task of finding a minimum for a given system's total Gibbs free energy. The advanced fuels are frequently multicomponent and heterogeneous systems. Therefore, it is pertinent to determine reasonable solution models in assessing the thermochemical behavior of metallic and nitride fuels. Thermochemical models have been made for phases expected in the advanced fuels. For metallic fuels, such models can predict alloying behaviors, the redistribution of materials and the reaction of the fuel with the cladding. In the case of nitride fuels, the models make it possible to forecast the vaporization of elements at elevated temperatures (e.g., reactor transients). The models would be also useful for the optimization of fabrication processes such as the carbothermic synthesis of the nitrides.

3.1. Actinide alloys

3.1.1. Alloys among actinides

There is a substantial database for the alloying behavior of uranium and plutonium [8]. The integral fast reactor (IFR) concept of the Argonne National Laboratory [9] revived interest in the use of metallic fuels in combination with pyrochemical or pyrometallurgical processes. The use of nitride fuels would require ^{15}N-enriched nitrogen and pyrochemical reprocessing makes it feasible to recycle the ^{15}N. The economical availability of ^{15}N-enriched nitrogen is not clearly known and metallic fuels remain as important alternatives.

Thermochemical models of U–Pu–Zr fuels have been proposed by several authors and applied to technical problems [10–14]. The U–Zr model [13], for instance, proved to give appropriate thermodynamic factors in analyzing the interdiffusion behavior of the alloys [15].

The integral molar free energy of a phase is given as

$$G_j = \sum_i X_i G_i^0 + G_{\text{ideal}}^0 + G_{\text{excess}}^0,$$

where the first term is the contribution from the pure elements, X_i is the atomic fraction of the element i taking the atomic arrangement of phase j and G_{ideal}^0 $(= -TS_{\text{ideal}})$ is that from the ideal entropy of mixing. Normally, G_i^0 is rather well-defined and the question is how to estimate the value of G_{excess}^0 the excess free energy. One approach is to find an appropriate set of free energy equations by combining experimental information of the phase diagram and thermodynamic properties to obtain the most plausible phase diagram and thermodynamic database for the given system. The above mentioned U–Pu–Zr models have been made in this way. This approach, assisted with a free-energy minimization computer code, is particularly useful in extrapolating the previous information to uninvestigated ranges. It does not, however, concern the underlying physics in alloying behavior and it is inadequate in the field where the experimental information is scarce or totally lacking, which is often the case with MA.

In terms of the technological importance as well as the interest in the fundamental alloying chemistry, a systematic study of neptunium alloys has been made by Gibson, Haire and co-workers [16–18]. Their work proved that the mutual solubility between Np and Am is limited. In the context of the metallic fuel concepts, the alloying behavior among actinides is particularly important.

The thermochemical predictions have been made with the Brewer model [19]. According to the recent physical theory [20], the enthalpy of formation of the transition-metal binary alloy is explained by the change in the width and filling of the common d-band formed between the two metals:

$$\Delta H_{\text{f}} = \Delta H_{\text{bond integral}} + \Delta H_{\text{bond order}}.$$

The Brewer model gives semi-empirical parameters roughly corresponding to those terms, although it is hard to establish exact one-to-one correspondence between the two concepts. The first term of the above physical concept is a positive term due to the change in bond lengths. On the other hand, by the terminology of the Brewer model, which has been borrowed from the model on the non-electrolyte solutions, a positive term comes from the internal pressure difference. The internal pressure is defined as E_{coh}/V. E_{coh} is the cohesive energy identified as the atomization energy of the element to a hypothetical valence state, which is supposed to exist in the elemental metal. V is the atomic volume. Both E_{coh} and V change with the crystal structure. The Brewer model also tells us where we would expect a significant contribution of $\Delta H_{\text{bond order}}$, which is due to the change in the d-band filling at the formation of the common band. For instance,

Table 1
Redlich–Kister–Muggianu-type polynomial coefficients for alloys of U, Np, Pu and Am [23]. The first element of the pair should be regarded as the element i in the equation. The parameters for U–Pu are estimated by fitting to the phase diagrams

Phase	Atomic pair	A^0 (J/mol)	A^1 (J/mol)
Liquid	U–Np	76.5	−1.94
	U–Pu	0	0
	U–Am	23982	3507
	Pu–Np	10614	−549
	Pu–Am	1177	141.5
	Np–Am	20661	3531
bcc	U–Np	177	−3.5
	U–Pu	3600	−1300
	U–Am	27055	4457
	Pu–Np	11975	−735
	Pu–Am	1026	127.1
	Np–Am	22072	4059
fcc	U–Np	960	−19.0
	U–Pu	3600	−1300
	U–Am	30114	4961
	Pu–Np	9866	−1038
	Pu–Am	1280	102.7
	Np–Am	19091	3511

Table 2
Free energies of transformation

Element	Transformation	ΔG_t (J/mol)
U	bcc/liquid	$9142-6.485T$
Np	bcc/liquid	$5188-5.69T$
Pu	bcc/liquid	$2824.2-3.093T$
	fcc/bcc	$1926-2.554T$
Am	bcc/liquid	$14393-9.933T$
	fcc/bcc	$5862-4.343T$

we would expect the largest negative $\Delta H_{\text{bond order}}$ by mixing a metal with nearly empty d-band and another with nearly filled d-band. It is because the cohesion given by the d-band is the largest when it is half-filled. However, there appears no simple method to accurately estimate $\Delta H_{\text{bond order}}$.

As for the alloys among actinides, we may neglect $\Delta H_{\text{bond order}}$ as the first approximation. On the other hand, besides the d-band, the 5f band plays an important role. The f-bonding contribution to the total cohesion of actinide metals has been estimated by Brewer [21], which, however, seems to be at variance with that later calculated by Brooks et al. [22] by a quantum-mechanical method. Nevertheless the application of Brewer model to the binary alloys among actinides gave provisional phase diagrams which are consistent with the recent experimental evidences [23].

Tables 1 and 2 show the parameters for calculating the binary and ternary alloy systems among U, Np, Pu and Am with the Redlich–Kister–Muggianu formulation:

$$\Delta G^0_{\text{excess}} = \sum_{i=1}^{n-1} \sum_{j=i+1}^{n} \sum_{p=0}^{m_{ij}} A^p_{ij} X_i X_j (X_i - X_j)^p,$$

where n is the number of components, m_{ij} is the degree of the polynomial for A^p_{ij}, A^p_{ij} is the pth polynomial coefficient for a binary pair i–j and X_i is the molar fraction of the component i. Here the interaction is assumed to be the first degree, i.e., $m_{ij} = 1$. In applying these parameters, the fcc phase has to be suppressed in calculating Pu–U, Np–U and Np–Pu binaries. This artificiality was imposed, as it is

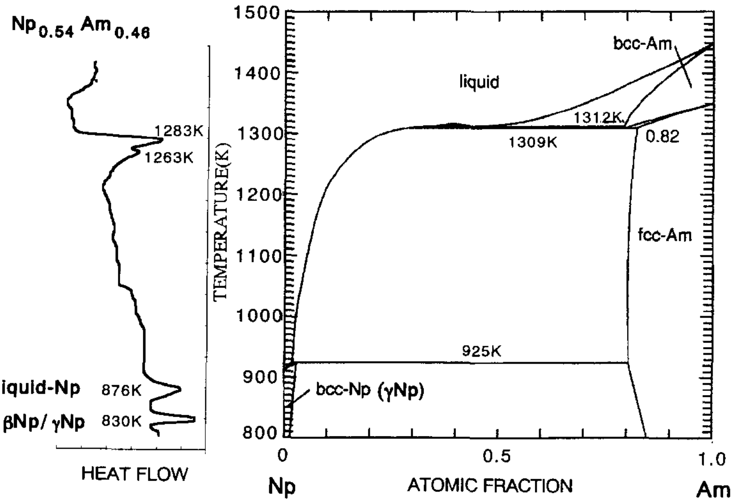

Fig. 4. Comparison of model prediction of Np–Am system with DTA measurement on $Np_{0.54}Am_{0.46}$ alloys. The DTA curve is shifted so as to place the peak maximums to the onset temperatures for the ease of comparison.

difficult to make accurate determination of the lattice energies, or the free energy of transformation (ΔG_t), of hypothetical phases of these heavy elements.

In the DTA measurements on a 54 at.% Np–46 at.% Am sample, the enthalpy peaks corresponding three allotropic transformations of Np (two of the three are shown in Fig. 4) were observed [16–18]. At higher temperatures there were two additional peaks, which were ascribed to the β(fcc)–γ transition and fusion of the Am-rich phases, respectively. The β–γ transition was depressed by ~ 60 K and the fusion by ~ 150 K from those of pure Am, giving rise to a narrow doublet at 1253–1293 K. On the other hand, the thermochemical model suggested a monotectic system with a barely discernible liquid miscibility gap: Two narrowly spaced horizontals at ~ 1310 K, which correspond to the observed doublet in the DTA curve, were noted. Another feature is the larger solubility of Np into Am than for the reverse case. Although the model gave a peritectic reaction at the Np-rich end, the DTA suggests that there is a eutectic for the Np-rich region.

The application of the Brewer model to Am alloys also revealed the essential immiscibility between U and Am [23]. Thus a metallic fuel based on U–Pu–Zr alloys with larger concentrations of Am, or on Np–Am alloys, is not likely to be a good choice for ABR.

3.1.2. Stability of ω-like intermediate phase

An inherent difficulty in determining phase diagrams for the actinide alloys has been identified. It is often difficult to control gaseous impurities in these alloys and this becomes more serious with minor actinides where one has to use smaller samples due to radiological concerns. The effect of nitrogen impurities on the equilibrium in the U–Zr system has been studied [24], where it was found that nitrogen destabilizes the bcc phase and the related intermediate phase, δ-UZr_2 (Fig. 5). This is one of the reasons why it is difficult to accurately determine the stability range of the δ-phase.

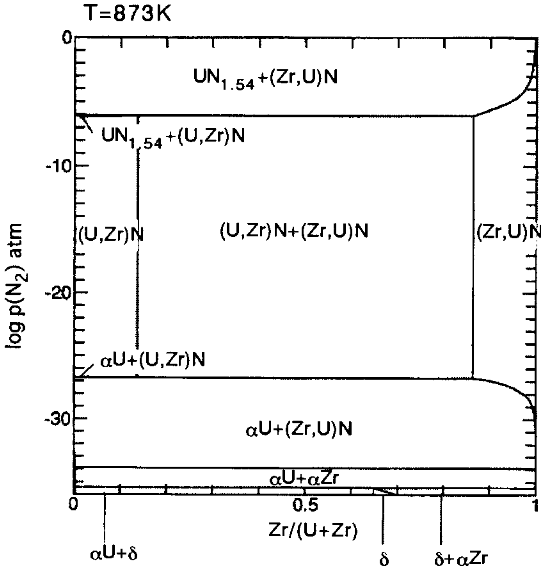

Fig. 5. Constitution of U–Zr–N alloys at 873 K as a function of nitrogen partial pressure. The δ solid solutions are destabilized by nitrogen.

Table 3

Parameters for modeling mixed nitrides ΔG_f^0 refers to the pure metal elements in liquid states, except for zirconium which refers to the α(hcp) phase. Species MV is hypothetical, which corresponds to the nitride with completely vacant non-metal sublattice. Definition of Redlich–Kister–Muggianu-type polynomial coefficients for ZrN–ZrV pair is as previously defined for metallic alloys. Parameters for americium are provisional, which were assumed to explain the vaporization behavior of ^{241}Am in PuN

Species	ΔG_f^0 (J/mol)	
Solid UN	$-306089+94.278T$	
Solid UV	$-13279+10\,631T$	
Liquid UN	$-251208+76\,71T$	
Liquid UV	0	
Solid PuN	$-296691+84.366T$	
Solid PuV	$-4770+5.69T$	
Liquid PuN	$-244091+66.796T$	
Liquid PuV	0	
AmN	$-297659+92.054T$	
AmV	0	
ZrN	$-367355+93.789T$	
ZrV	3350	
Pair	**L (J/mol)**	**Remark**
UV–UN (solid)	$10000+20T$	
UV–UN (liquid)	$84500-17T$	
PuV–PuN (solid)	$-60800+46.4T$	
PuV–PuN (liquid)	$-84000+45T$	
AmV–AmN	0	
UV–PuV	0	
UN–PuN	0 or $38000-30T$	 see Ref. [32]
PuV–AmV	0	
PuN–AmN	0	
ZrV–ZrN	L^0: 0 L^1:40000	
ZrN–UN	18410	
ZrV–UV	$36200+4.216T$	

Correct information on the stability of δ-UZr_2 is important, as it is a phase encountered in U–Pu–Zr fuels and controls the material redistribution under the radial thermal gradient in the fuel element [14]. In addition, a very similar phase has been identified in Np–Zr alloys [25]. The lattice stability of δ-UZr_2 has been studied by thermal analysis and its structure determined by neutron diffraction [26]. It was confirmed that the crystal structure is a modified C32 structure like the ω-phase, known as a metastable phase of Zr-based alloys. In the U–Zr system, the atomic volume increases at the transition from δ to (γ-U, β-Zr): the δ phase has a dense structure like the ω-phase with respect to the bcc structure. Thus, the δ-phase may be regarded as a series of ω-phase solid solutions. The heat effects at the transition were extrapolated to $X_{Zr} = 1$ to give ΔH_t(ω-Zr/β-Zr) = 2800 J/g atom, which supports the previous estimate from the phase diagram analysis: ΔH_t(ω-Zr/β-Zr) = 3094 J/g atom [13].

3.2. Actinide nitrides

3.2.1. Mixed nitrides of actinides

The nitride fuels have thermal conductivities comparable to metallic fuels and high melting points (~ 3000 K) [27]. The good thermal properties of nitrides and carbides provide the unique possibility of using them as 'cold fuel' even at a high linear heating rate [28]. Another potential advantage is the mutual solubility expected for actinide mononitrides. The carbide fuels are not considered as candidates for ABR, since the carbides of transplutonium elements are not sufficiently stable [29]. It has been shown, however, that UN and (U, Pu)N decompose at high temperatures to form liquid phases, which sets an operational limit of the fuels [30].

Vaporization behaviors of hypostoichiometric nitrides have been calculated [31–33]. The properties of MN_{1-x} have been modeled with a sublattice formalism, where nitrogen and its vacancy occupy a non-metal sublattice of the NaCl-type structure. The excess free energy of mixing is then given as a function of site occupation fractions, Y_{Mi} and Y_{Nj}, on the metal and non-metal sublattices, respectively:

$$\Delta G^0_{\text{excess}} = \sum_{i=1}^{2} Y_{Mi} L_{Ni} Y_{N1} Y_{N2} + \sum_{j=1}^{2} Y_{Nj} L_{Mj} Y_{M1} Y_{M2},$$

$$Y_{N1} + Y_{N2} = 1,$$

$$Y_{M1} + Y_{M2} = 1,$$

where the Ls are the regular interaction parameters: L_{Ni} for the non-metal and L_{Mj} for the metal sublattices, respectively. The pertinent parameters are given in Table 3.

One important result of such an analysis is that one cannot predict the behaviors for a series of solid solutions of UN–PuN by treating them as pseudo-binary systems [32]. There is a congruent vaporization of Pu and N_2 near the PuN-rich end, whereas nitrogen is preferentially lost near the UN-rich end. Thus, the concentration of structural vacancy changes with the Pu/(U + Pu) ratio.

The same theoretical treatment has been applied to the vaporization of ^{241}Am, the daughter of ^{241}Pu, which is found in reactor-grade PuN [33]. An unusual vaporization behavior was noted for a sample of reactor-grade PuN that contained ~ 1.3 at.% Am. Initially the mass-239 signal was much lower than the thermodynamic expectation, while the mass-241 signal was significantly large. After continued heating the mass-241 signal subsided and the mass-239 signal increased to a stable level. A subsequent analysis of the data revealed that the vaporization of (Pu, Am)N consists of three stages: (1) preferential loss of N_2, (2) preferential loss of Am and N_2 and (3) congruent vaporization of PuN. The partial pressure of Pu in the third stage followed exactly that expected from data obtained with samples using purer PuN. The second-law enthalpy of formation of AmN was estimated from the partial pressures of Am in the third stage: an enthalpy of −294 kJ/mol was obtained at the average temperature of 1600 K, which is comparable to $\Delta H^0_{f,298} = -296$, −299 and −301 kJ/mol for UN [34], PuN [34] and LaN [35], respectively. A high vapor pressure of Am over AmN has an important practical implication, which is discussed further in Ref. [36].

3.2.2. Uranium zirconium nitrides

The mixed nitrides with ZrN are of interest, since the addition of ZrN would suppress vaporization of the actinides [37]. Therefore, ZrN may be a reasonable choice as diluting matrix for the actinide burning. The interaction parameter for the UN–ZrN pair (Table 3) is as estimated by Holleck and Ishii [38], who used an empirical correlation between the interaction parameter and the lattice parameter difference of the components. This correlation was based on data for mixed carbides. The interaction parameter gives a critical point of 1073 K for the miscibility gap of UN–ZrN. However, miscibility of those refractory materials at lower temperatures is difficult to define experimentally.

A sample of U–18 at.% Zr alloy was heated at 1273 K under a low-pressure N_2 [39]. The scale was formed on the alloy, which was found to consist of two layers: a very thin (< 1 μm) layer of (U, Zr)N at the surface on a thick layer of α-Zr(N) which covers the alloy. The Auger analysis revealed that the concentration of (U, Zr)N layer changed from ~ 80% UN near the surface to ~ 100% ZrN near the interface with α-Zr(N). The analysis did not show a significant concentration gap within the (U, Zr)N layer, suggesting complete miscibility at the temperature as expected from the above model.

References

[1] H. Murata, T. Mukaiyama, Atomkern-Energ. Kerntechn. 45 (1984) 23.

[2] T. Ogawa et al., in: Proc. Global, Int. Conf. on Evaluation of Emerging Nuclear Fuel Cycle Systems, Versailles, France, Sept. 11–14, French Section of American Nuclear Society, 1995, pp. 207–214.

[3] T. Osugi et al., in: Proc. Global, Int. Conf. Evaluation of Emerging Nuclear Fuel Cycle Systems, Versailles, France, Sept. 11–14, French Section of American Nuclear Society, 1995, pp. 181–189.

[4] F. Kobayashi, J. Am. Ceram. Soc. 78 (1995) 2279.

[5] M. Handa et al., JAERI-RDIPE Seminar on Lead Cooled Fast Reactor, Oct. 28–29, 1983.

[6] M. Akabori, A. Itoh, T. Ogawa, paper presented at International Symposium on Interfacial Effects in Quantum Engineering Systems (IEQES-96), Mito, Japan, Aug. 21–23, 1996.

[7] T. Ogawa, F. Kobayashi, Japanese patent application H8-164604, 1996.

[8] P. Chiotti et al., The Chemical Thermodynamies of Actinide Elements and Compounds, Pt 5: The Actinide Binary Alloys (IAEA, Vienna, 1981).

[9] Y.I. Chang, C.E. Till, in: LMR: A Decade of LMR Progress and Promise (American Nuclear Society, La Grange Park, IL, 1991).

[10] L. Leibowitz et al., J. Nucl. Mater. 154 (1988) 145.

[11] L. Leibowitz, R.A. Blomquist, A.D. Pelton, J. Nucl. Mater. 167 (1989) 76.

[12] L. Leibowitz, R.A. Blomquist, A.D. Pelton, J. Nucl. Mater. 184 (1991) 59.

[13] T. Ogawa, T. Iwai, J. Less Common Met. 170 (1991) 101.

[14] T. Ogawa, T. Iwai, M. Kurata, J. Less Common Met. 175 (1991) 59.

[15] T. Ogata, M. Akabori, A. Itoh, T. Ogawa, J. Nucl. Mater. 232 (1996) 125.

[16] J.K. Gibson, R.G. Haire, J. Nucl. Mater. 195 (1992) 156.

[17] J.K. Gibson, R.G. Haire, M.M. Gensini, T. Ogawa, J. Alloys Compounds 213&214 (1994) 106.

[18] J.K. Gibson, R.G. Haire, Y. Okamoto, T. Ogawa, J. Alloys Compounds 234 (1996) 34.

[19] L. Brewer, R.H. Lamoreaux, At. Energy Rev. 7 (1980) 11194, Special issue.

[20] D.G. Pettifor, in: Solid State Physics, eds. H. Ehrenreich and D. Turnbull, Vol. 40 (Academic Press, New York, 1987) p. 43.

[21] L. Brewer, Lawrence Berkley Laboratory Rept. LBL-3720, 1975.

[22] M.S.S. Brooks, B. Johansson, H.L. Skriver, in: Handbook on the Physics and Chemistry of the Actinides, eds. A.J. Freeman and G.H. Lander (Elsevier Science, Amsterdam, 1984) p. 153.

[23] T. Ogawa, J. Alloys Compounds 194 (1993) 1.

[24] T. Ogawa, M. Akabori, J. Alloys Compounds 213 (1994) 173.

[25] Y. Okamoto, R.G. Haire, J.K. Gibson, T. Ogawa, J. Alloys Compounds 232 (1996) 302.

[26] M. Akabori, T. Ogawa, A. Itoh, Y. Morii, J. Phys. 7 (1995) 8249.

[27] Hj. Matzke, Science of Advanced LMFBR Fuels (North-Holland, Amsterdam, 1986).

[28] H. Blank, J. Less Common Met. 121 (1986) 583.

[29] C.E. Holley Jr., M.H. Rand, E.K. Storms, The Chemical Thermodynamics of Actinide Elements and Compounds, Pt 6: The Actinide Carbides (IAEA, Vienna, 1984).

[30] K. Richter, C. Sari, J. Nucl. Mater. 184 (1991) 167.

[31] T. Ogawa, J. Alloys Compounds 203 (1994) 221.

[32] T. Ogawa, J. Nucl. Mater. 201 (1993) 284.

[33] T. Ogawa, T. Ohmichi, A. Macda, Y. Arai, Y. Suzuki, J. Alloys Compounds 224 (1995) 55.

[34] T. Matsui, R.W. Ohse, High Temp. High Press. 19 (1987) 1.

[35] K.A. Gschneidner Jr., N. Kippenhan, Iowa State University Rep. IS-RIG-5, 1972.

[36] T. Ogawa, Y. Shirasu, K. Minato, H. Serizawa, these Proceedings, p. 151.

[37] R.A. Potter, J.L. Scott, Deut. Offenlegungsschrift 2532739, 1976.

[38] H. Holleck, T. Ishii, Kernforschungszentrum Karlsruhe Rep. KFK 1754, 1973.

[39] A. Itoh, M. Akabori, T. Ogawa, paper to be presented at 1996 Fall Meeting of the Atomic Energy Society of Japan.